Performance Analysis of Cellular Edge Users with Air-Ground Cooperation

Ruiyun Wu*†, Na Deng*†, Martin Haenggi‡, Haichao Wei§, and Nan Zhao*
*School of Information and Communication Engineering, Dalian University of Technology, Dalian 116024, China
†State Key Laboratory of Integrated Services Networks (Xidian University), Xi'an, 710071, China
‡Dept. of Electrical Engineering, University of Notre Dame, Notre Dame, IN 46556, USA
§School of Information Science and Technology, Dalian Maritime University, Dalian 116026, China
Email: wury2022@mail.dlut.edu.cn, {dengna, zhaonan}@dlut.edu.cn, mhaenggi@nd.edu, weihaichao@dlmu.edu.cn

***Abstract*—To address the poor performance experienced by cell-edge users located equidistantly to the serving base station (BS) and the nearest interfering BS(s), this paper proposes an air-ground coordinated multipoint scheme assisted by unmanned aerial vehicles and the dynamic coordinated BSs selected from the sets of the serving and the equidistant interfering BSs. Using stochastic geometry tools, we derive success probabilities in a Poisson cellular network for the users located at corners of the Voronoi diagram called worst-case users served using non-coherent joint transmission. To reflect the impact of the coordinated transmission on the overall network performance, we also deduce the normalized spectral efficiency. Numerical results validate the accuracy of our analytical findings and show the superior performance of the proposed scheme for the worst-case users.**

I. Introduction

As mobile communication continues to advance and diverse applications emerge, user demands for transmission reliability and capacity have grown significantly. For instance, 5G enhanced mobile broadband (eMBB) users seek high transmission rates, while ultra-reliable and low-latency communication (URLLC) users prioritize extremely reliable transmission. However, cell-edge users located far away from base stations (BS) suffer from weak desired signals and severe interference from neighboring BSs in large-scale cellular networks, resulting in low quality of service (QoS) [1]. Consequently, addressing the needs of these cell-edge users has become imperative, as they become a performance bottleneck within the network.

To enhance the performance for cell-edge users, coordinated multipoint (CoMP) of ground BSs is a pivotal solution. The works of [2, 3] presented a tractable stochastic geometry-based model to analyze the benefits of joint BS transmission for both general and cell-corner users. In [4], the authors proposed a location-dependent BS cooperation scheme in non-coherent joint transmission manner for the users located at different regions, and stochastic geometry approach is also used to evaluate the performance improvement. However, the BSs participating in the coordinated transmission need to reserve the common idle resources. This means that these BSs cannot serve their own users using the reserved resources, potentially impacting the overall spectrum efficiency of the network. In order to solve this problem, new technologies have emerged to facilitate coordinated transmissions, such as intelligent reflecting surfaces (IRS) and unmanned aerial vehicles (UAV). In [5], the authors explored an IRS-aided joint CoMP transmission to assist BS in serving cell-edge users and aiming to maximize the minimum achievable rate for these users. However, deploying IRS systems can entail additional costs and offer limited flexibility. Fortunately, the emergence of UAV technology presents a promising and flexible solution to overcome these limitations. In [6], multiple UAVs assisted users and a joint optimization problem was formulated to minimize the aggregate gap between the target rates and the actual user rates via optimizing the 3D positions of the UAV BSs and network resources within a single-cell scenario. The article [7] used a Gauss-Poisson process to model the locations of BSs and UAVs, with a specific focus on the performance of a general user jointly served by a pair of BS and UAV. Furthermore, considering the users located in malfunction areas where BSs are out of order, the authors in [8] proposed a user-centric cooperative scheme to serve the users using stochastic geometry tools. However, they focus on the general user located arbitrarily in the whole network, and the resulting performance is averaged over all the possible locations, which conceals the performance characteristics of cell-edge users. To the best of our knowledge, the use of UAV-BS CoMP for enhancing the QoS of cell-corner users remains unexplored.

In this paper, we propose an air-ground cooperation scheme characterized by the UAV flexibility and allowing a dynamic number of nearby BSs to help users located at the cell corners. Different from the existing schemes with a fixed number of cooperators, our scheme is more general with dynamic cooperation levels to improve the performance of edge users while minimizing the impact on the quality of service in the neighboring cells. Specifically, a Poisson point process (PPP) is used to model locations of BSs. For the target users located at the vertices of the Voronoi diagram, we propose to deploy UAVs directly over these users, and non-coherent joint transmission between the serving UAV and part of the equidistant nearest BSs is adopted to enhance the user-perceived performance. For this setup, we derive the success probabilities for worst-case users with different coordinated BS sets to

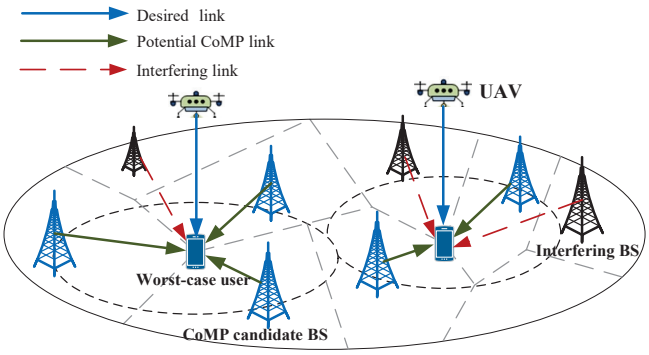

Fig. 1. An example of air-ground cooperation scheme

characterize the user-perceived performance. The normalized spectral efficiency is also analyzed to reflect the cost of coordination. Numerical results demonstrate the accuracy of the derived expression and highlight the superior performance of our proposed scheme in terms of success probability and normalized spectrum efficiency in comparison with the three-BS CoMP and no CoMP schemes.

II. System Model

A. Network Model

We consider a UAV-assisted cellular downlink network and model the locations of BSs as a homogeneous PPP $\Phi=\{x_1, x_2, \cdots\}$ of density λ in the Euclidean plane $\mathbb{R}^2$. Each BS has a transmit power of $\mu_{\rm b}$ and is equipped with an omnidirectional antenna. We focus on the worst-case users, which are located at the Voronoi corners and have three equidistant BSs. When randomly choosing one as the serving BS, these users experience severe interference from the two other equidistant BSs and can be regarded as the worst-case users from a geometric point of view [4, 9]. To enhance the QoS of these worst-case users, we assume that UAVs are deployed over the vertices of the Voronoi diagram at a height of h to serve as aerial BSs, and the projection locations of UAVs are the set of all the Voronoi vertices. According to [10, Tier 3], the UAVs then form a stationary point process with density 2λ. We further assume that each UAV adopts a downward narrow beam pointing to the target user below and has a transmit power of $\mu_{\rm u}$. In addition, the ground BSs and the UAVs share the spectrum resources.

B. Air-ground Cooperation Scheme

Although the UAV can enhance the desired signal strength, the interference from the surrounding BSs still hurts the QoS of the worst-case users, especially from the equidistant interfering BSs. Furthermore, the signal power of the UAV depends on its height, which is constrained by the realistic environments and the regulations of the government and industrial association [11]. Hence, we propose a flexible air-ground cooperative transmission scheme to further enhance the performance of the worst-case users, where the three equidistant nearest BSs are natural candidates for the cooperation with the UAV, as shown in Fig. 1. The non-coherent joint transmission scheme in [12] is adopted for the coordinated BSs and the UAV to serve the worst-case user. Conditioning on a Voronoi vertex to be at the origin, we consider a user located at the origin served by the proposed cooperative scheme, who becomes the typical worst-case user after averaging over Φ. Letting $\mathcal{V}=\{x_1, x_2, x_3\}$ be the three equidistant BSs closest to the typical worst-case user, they could participate in the cooperative transmission according to their user loads, and the coordinated BS set, denoted by $\mathcal{W}\subseteq\mathcal{V}$. The number of coordinated BS is denoted by $N=\#\mathcal{W}\in\{1,2,3\}$.

C. Channel Model

We consider two types of channel models, the terrestrial channel from a BS to a user and the air-to-ground channel from the serving UAV to a user. Both channels are characterized by large-scale path loss and small-scale fading. For the terrestrial channel, the path loss model is $\ell(x)=\|x\|^{-\alpha_{\rm b}}$, where $\alpha_{\rm b}$ is the path loss exponent, and we consider Rayleigh fading, i.e., the power fading coefficient from BS x to the typical user, denoted by g_x, follows an exponential distribution with unit mean.

Since the UAV is directly above the target user, we assume a line-of-sight (LOS) propagation and adopt the Nakagami fading model. In this case, the power fading coefficient follows $g_{\rm u}\sim\text{gamma}(m,1/m)$, where $m>1$ represents the Nakagami parameter. The path loss model of the air-to-ground channel is $h^{-\alpha_{\rm u}}$, where $\alpha_{\rm u}\leq\alpha_{\rm b}$. Additionally, due to the narrow beam pointed at the user below of each UAV, the interference caused by the other UAVs is negligible.

Under the non-coherent joint transmission in [12], the received signal-to-interference ratio (SIR) at the typical worst-case user can be expressed as

$$\text{SIR}=\frac{\mu_{\rm u}h^{-\alpha_{\rm u}}g_{\rm u}+\mu_{\rm b}\sum\limits_{x\in\mathcal{W}}\ell(x)g_x}{I_{\rm eq}+I_{\rm re}},\tag{1}$$

where $I_{\rm eq}$ is the interference from the $3-N$ equidistant interfering BSs in $\mathcal{V}\setminus\mathcal{W}$, and $I_{\rm re}$ is the interference from the remaining interfering BSs, respectively expressed by

$$\begin{aligned}I_{\rm eq}&=\mu_{\rm b}\sum_{x\in\mathcal{V}\setminus\mathcal{W}}g_x\ell(x)\\ I_{\rm re}&=\mu_{\rm b}\sum_{x\in\Phi\setminus\mathcal{V}}g_x\ell(x),\end{aligned}\tag{2}$$

and $I=I_{\rm eq}+I_{\rm re}$ represents the aggregated interference.

III. Performance Analysis

In this section, we will use the success probability and the normalized spectral efficiency as the criteria to evaluate the performance of the proposed scheme.

A. Success Probability

The success probability is defined as the complementary cumulative distribution function (CCDF) of the SIR, given by

$$P_{\rm s}(T)=\mathbb{P}(\text{SIR}>T),\tag{3}$$

where T denotes the SIR threshold. To derive the success probability, we need the probability distribution of the distance from worst-case users to the serving BSs. Let D be the distance from the typical worst-case user to the serving BS, i.e., $D = \|x_1\| = \|x_2\| = \|x_3\|$. The probability density function (PDF) of D for the typical worst-case user is given by [9]

$$f_D(t) = 2(\lambda\pi)^2 t^3 \exp(-\lambda\pi t^2), t \geq 0. \tag{4}$$

Then we can obtain the expectation of the serving distance as

$$\mathbb{E}D = \int_0^\infty 2(\lambda\pi)^2 t^4 \exp(-\lambda\pi t^2)\mathrm{d}t = \frac{\Gamma(2.5)}{(\lambda\pi)^{0.5}}. \tag{5}$$

Subsequently, we present the key intermediate results concerning the conditional Laplace transform of the interference given $D = t$ and its derivatives in the following lemma.

Lemma 1. *Given the serving distance $D = t$, the Laplace transform of the aggregated interference $I(t)$ for the typical worst-case user is given by $\mathcal{L}_I(s,t) = \mathcal{L}_{I_{\mathrm{eq}}}(s,t)\mathcal{L}_{I_{re}}(s,t)$, where*

$$\mathcal{L}_{I_{\mathrm{eq}}}(s,t) = \Big(\frac{1}{1+\mu_{\mathrm{b}} s t^{-\alpha_{\mathrm{b}}}}\Big)^{3-N},$$
$$\mathcal{L}_{I_{\mathrm{re}}}(s,t) = \exp\left(-2\pi\lambda\int_t^\infty \frac{r}{1+\mu_{\mathrm{b}}^{-1}s^{-1}r^{\alpha_{\mathrm{b}}}}\mathrm{d}r\right). \tag{6}$$

The n-th derivative of $\mathcal{L}_I(s,t)$ w.r.t. s is given by

$$\mathcal{L}_I^{(n)}(s,t) = \sum_{k=0}^{n}\binom{n}{k}\mathcal{L}_{I_{\mathrm{re}}}^{(n-k)}(s,t)\cdot\mathcal{L}_{I_{\mathrm{eq}}}^{(k)}(s,t), \tag{7}$$

where

$$\mathcal{L}_{I_{\mathrm{eq}}}^{(n)}(s,t) = \frac{\big(-\mu_{\mathrm{b}}t^{-\alpha_{\mathrm{b}}}\big)^n}{\big(1+\mu_{\mathrm{b}}s\ell(t)\big)^{3-N+n}}\frac{\Gamma(n+3-N)}{\Gamma(3-N)},\ n>0 \tag{8}$$

$$\mathcal{L}_{I_{\mathrm{re}}}^{(n)}(s,t) = \sum_{k=0}^{n-1}\binom{n-1}{k}\eta^{(n-k)}(s,t)\cdot\mathcal{L}_{I_{\mathrm{re}}}^{(k)}(s,t), n>0, \tag{9}$$

$$\eta^{(k)}(s,t) = 2\pi\lambda(-\mu_{\mathrm{b}})^k\Gamma(1+k)\int_t^\infty \frac{r^{1-k\alpha_{\mathrm{b}}}}{(1+\mu_{\mathrm{b}}sr^{-\alpha_{\mathrm{b}}})^{k+1}}\mathrm{d}r. \tag{10}$$

Proof: See Appendix A.

Next, we provide the probability distribution of the desired signal power received by the typical worst-case user, denoted by S, which is a sum of $N+1$ gamma random variables, expressed as

$$S = \mu_{\mathrm{u}}h^{-\alpha_{\mathrm{u}}}g_{\mathrm{u}} + \mu_{\mathrm{b}}D^{-\alpha_{\mathrm{b}}}\sum_{x\in\mathcal{W}} g_x. \tag{11}$$

Since g_{u} follows a gamma distribution with parameters $(K = m, \theta = 1/m)$, we obtain

$$\mu_{\mathrm{u}}h^{-\alpha_{\mathrm{u}}}g_{\mathrm{u}} \sim \mathrm{gamma}\Big(K_{\mathrm{u}} = m, \theta_{\mathrm{u}} = \frac{\mu_{\mathrm{u}}h^{-\alpha_{\mathrm{u}}}}{m}\Big). \tag{12}$$

Similarly, due to $g_x \sim \mathrm{gamma}(K=1,\theta=1)$, we have

$$\mu_{\mathrm{b}}D^{-\alpha_{\mathrm{b}}}g_x \sim \mathrm{gamma}\big(K_x = 1, \theta_x = \mu_{\mathrm{b}}D^{-\alpha_{\mathrm{b}}}\big). \tag{13}$$

To achieve a tractable approximation of a sum of $N+1$ gamma random variables, we adopt the second-order moment matching method, which has only a small margin of error [13]. Therefore, a new gamma random variable $J \sim \mathrm{gamma}(K,\theta)$ is introduced to approximate the exact desired signal strength S, where the parameters K, θ depend on the serving distance D as

$$K(D) = \frac{m(\mu_{\mathrm{u}}h^{-\alpha_{\mathrm{u}}} + N\mu_{\mathrm{b}}D^{-\alpha_{\mathrm{b}}})^2}{(\mu_{\mathrm{u}}h^{-\alpha_{\mathrm{u}}})^2 + mN(\mu_{\mathrm{b}}D^{-\alpha_{\mathrm{b}}})^2}, \tag{14}$$

$$\theta(D) = \frac{(\mu_{\mathrm{u}}h^{-\alpha_{\mathrm{u}}})^2 + mN(\mu_{\mathrm{b}}D^{-\alpha_{\mathrm{b}}})^2}{m(\mu_{\mathrm{u}}h^{-\alpha_{\mathrm{u}}} + N\mu_{\mathrm{b}}D^{-\alpha_{\mathrm{b}}})}. \tag{15}$$

It can be obtained that $\mathbb{E}(J) = K\theta = \mu_{\mathrm{u}}h^{-\alpha_{\mathrm{u}}} + N\mu_{\mathrm{b}}D^{-\alpha_{\mathrm{b}}}$ is the mean received power from all cooperators and that the variance $\mathrm{var}(J) = K\theta^2 = (1/m)(\mu_{\mathrm{u}}h^{-\alpha_{\mathrm{u}}})^2 + N(\mu_{\mathrm{b}}D^{-\alpha_{\mathrm{b}}})^2$ is the squared mean powers scaled by $1/m$ and N, respectively.

After calculating the parameters of J and the conditional Laplace transform $\mathcal{L}_I(s,t)$, the success probability of the worst-case user can be obtained in the following theorem.

Theorem 1. *Letting $\bar{K} \triangleq \mathbb{E}(K(D))$, the success probability for the typical worst-case user is approximated as*

$$P_{\mathrm{s}}(T) \approx \sum_{n=1}^{\infty}\binom{\bar{K}}{n}(-1)^{n+1}\int_0^\infty f_D(t)\mathcal{L}_I\Big(\frac{n\bar{\xi}T}{\theta(t)}, t\Big)\mathrm{d}t, \tag{16}$$

where $\bar{\xi} = (\Gamma(1+\bar{K}))^{-1/\bar{K}}$.

Proof: With the distance distribution and the Laplace transform of $I(t)$, the success probability is given by

$$\begin{aligned}
P_{\mathrm{s}}(T) &= \mathbb{P}(S > TI)\\
&\approx \mathbb{E}_D\big[\mathbb{P}(J > TI(t)) \mid D\big]\\
&= \int_0^\infty \mathbb{P}(J > TI(t))f_D(t)\mathrm{d}t\\
&= \int_0^\infty \mathbb{E}\Big[\widetilde{\Gamma}\Big(K(t), \frac{TI(t)}{\theta(t)}\Big)\Big]f_D(t)\mathrm{d}t\\
&\overset{(a)}{\geq} \int_0^\infty \mathbb{E}\left[1-\left(1-\exp\Big(-\frac{\xi(t)TI(t)}{\theta(t)}\Big)\right)^{K(t)}\right]f_D(t)\mathrm{d}t\\
&\overset{(b)}{\approx} \int_0^\infty \mathbb{E}\left[1-\left(1-\exp\Big(-\frac{\bar{\xi}TI(t)}{\theta(t)}\Big)\right)^{\bar{K}}\right]f_D(t)\mathrm{d}t\\
&\overset{(c)}{=} \int_0^\infty \mathbb{E}\left[\sum_{n=1}^{\infty}\binom{\bar{K}}{n}(-1)^{n+1}\exp\Big(\frac{-n\bar{\xi}TI(t)}{\theta(t)}\Big)\right]f_D(t)\mathrm{d}t\\
&= \int_0^\infty f_D(t)\sum_{n=1}^{\infty}\binom{\bar{K}}{n}(-1)^{n+1}\mathcal{L}_I\Big(\frac{n\bar{\xi}T}{\theta(t)}, t\Big)\mathrm{d}t,
\end{aligned} \tag{17}$$

where $\xi(t) = \big(\Gamma(1+K(t))\big)^{-1/K(t)}$ and step (a) follows from the tight upper bound for the normalized incomplete gamma function $\widetilde{\Gamma}(\cdot)$ in [14], given by

$$\begin{aligned}
\mathbb{P}(J > v) &= \widetilde{\Gamma}(K, v/\theta)\\
&\geq 1-\left(1-\exp\Big(-\big(\Gamma(1+K)\big)^{-\frac{1}{K}}\frac{v}{\theta}\Big)\right)^K,
\end{aligned}$$

with $J \sim \text{gamma}(K,\theta)$. Step (b) uses the approximation $\mathbb{E}f(D) \approx f(\mathbb{E}D)$ for simplification and step (c) follows from the generalized binomial theorem. ■

In Thm. 1, the infinite sum results in a high computational complexity since $K(t)$ and $\bar{K}$ are not integers. In the following, we first obtain an upper integer bound of the shape parameter K, which results in an approximate expression of the success probability with a finite sum.

Corollary 1. *The success probability for the typical worst-case user is approximated as*

$$P_{\rm s}(T) \approx \sum_{k=0}^{m+N-1} \int_0^\infty \frac{(-u)^k}{k!} \mathcal{L}_I^{(k)}(u,t)|_{u=\frac{T}{\theta(t)}} f_D(t){\rm d}t. \quad (18)$$

Proof: Letting $\mathbf{a}$ be a column vector with the i-th element $a_i = 1$ for $i = 1,\ldots,N+m$ and $\mathbf{b}$ be a column vector with $b_i = \frac{\mu_{\rm u} h^{-\alpha_{\rm u}}}{m}, i = 1,\ldots,m$ and $b_i = \mu_{\rm b} D^{-\alpha_{\rm b}}, i = m+1,\ldots,m+N$, we rewrite the numerator of $K(D)$ in (14) in the inner product form of $(\mathbf{a}^{\rm T}\mathbf{b})^2$. According to the Cauchy-Schwarz inequality, we have

$$\begin{aligned} K(D) &\le \frac{\left(\sum_{i=1}^{N+m} a_i^2\right) \times \left(\sum_{i=1}^{N+m} b_i^2\right)}{\frac{(\mu_{\rm u} h^{-\alpha_{\rm u}})^2}{m} + N(\mu_{\rm b} D^{-\alpha_{\rm b}})^2} \\ &= \frac{(m+N)\left[m\left(\frac{\mu_{\rm u} h^{-\alpha_{\rm u}}}{m}\right)^2 + N(\mu_{\rm b} D^{-\alpha_{\rm b}})^2\right]}{\frac{(\mu_{\rm u} h^{-\alpha_{\rm u}})^2}{m} + N(\mu_{\rm b} D^{-\alpha_{\rm b}})^2} \\ &= m+N. \end{aligned} \quad (19)$$

Using a gamma random variable $\tilde{J} \sim \text{gamma}(m+N, \theta(D))$ to approximate S, we have

$$\begin{aligned} P_{\rm s}(T) &= \mathbb{P}(S > TI) \\ &\approx \mathbb{E}_D\left[\mathbb{P}(\tilde{J} > TI(t)) \mid D\right] \\ &= \int_0^\infty \mathbb{E}\left[\widetilde{\Gamma}\left(m+N, \frac{TI(t)}{\theta(t)}\right)\right] f_D(t){\rm d}t \\ &= \int_0^\infty \sum_{k=0}^{m+N-1} \frac{1}{k!} \mathbb{E}\left[\left(\frac{TI(t)}{\theta(t)}\right)^k \exp\left(-\frac{TI(t)}{\theta(t)}\right)\right] f_D(t){\rm d}t \\ &= \int_0^\infty \sum_{k=0}^{m+N-1} \frac{(-u)^k}{k!} \mathcal{L}_I^{(k)}(u,t)|_{u=\frac{T}{\theta(t)}} f_D(t){\rm d}t. \end{aligned} \quad (20)$$

■

B. Normalized Spectral Efficiency

In order to evaluate the impact of the coordinated transmission on the overall network performance, the normalized spectral efficiency η defined in [4] is considered in this paper and expressed by

$$\eta \triangleq \frac{1}{N}\mathbb{E}\left[\ln(1+{\rm SIR})\right]. \quad (21)$$

The following theorem gives the normalized spectral efficiency of worst-case users with different N.

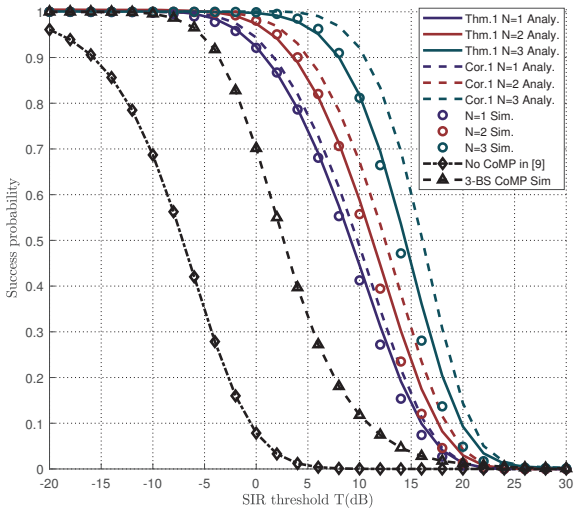

Fig. 2. The success probabilities versus T with different N.

Theorem 2. *The normalized spectral efficiency of the worst-case user is approximated as*

$$\eta \approx \frac{1}{N}\int_0^\infty\int_0^\infty \frac{f_D(t)}{\varepsilon+1} \sum_{n=1}^{\infty} \binom{\bar{K}}{n} (-1)^{n+1} \mathcal{L}_I\left(\frac{n\xi\varepsilon}{\theta}, t\right) {\rm d}\varepsilon{\rm d}t. \quad (22)$$

Proof: According to the definition of the normalized spectral efficiency, we have

$$\begin{aligned} \eta &= \frac{1}{N}\mathbb{E}\left[\ln\left(1+\frac{S}{I}\right)\right] \\ &= \frac{1}{N}\int_0^\infty\int_0^\infty \mathbb{P}\left(\ln\left(1+\frac{S}{I}\right) > v\right){\rm d}v f_D(t){\rm d}t \\ &\overset{(a)}{\approx} \frac{1}{N}\int_0^\infty\int_0^\infty \frac{1}{\varepsilon+1}\mathbb{P}(J > \varepsilon I){\rm d}\varepsilon f_D(t){\rm d}t \\ &\overset{(b)}{\approx} \frac{1}{N}\sum_{n=1}^{\infty}\int_0^\infty\int_0^\infty \binom{\bar{K}}{n} \frac{(-1)^{n+1} f_D(t)}{\varepsilon+1} \mathcal{L}_I\left(\frac{n\xi\varepsilon}{\theta(t)}, t\right){\rm d}\varepsilon{\rm d}t, \end{aligned} \quad (23)$$

where step (a) is obtained by replacing $e^v - 1$ with ε and step (b) is similar to the derivation of the success probability. ■

IV. NUMERICAL RESULTS

In this section, we give numerical results of the success probabilities for the worst-case users in air-ground cooperative networks. To show the effectiveness of the proposed air-ground cooperative scheme, we consider two benchmark schemes without UAV assistance: one is the no CoMP scheme where the worst-case user merely randomly chooses a nearest BS as the serving one in [9] and the other is the three-BS CoMP scheme where the worst-case user is served by the three equidistant nearest BSs using non-coherent joint transmission. Unless otherwise stated, the simulation parameters as follows: $h = 100$, $\alpha_{\rm b} = 4$, $\alpha_{\rm u} = 2.5$, $\mu_{\rm b} = 40$, $\mu_{\rm u} = 1$, $m = 3$ and $\lambda = 5 \times 10^{-5}$, which results in $\mathbb{E}D = 106$.

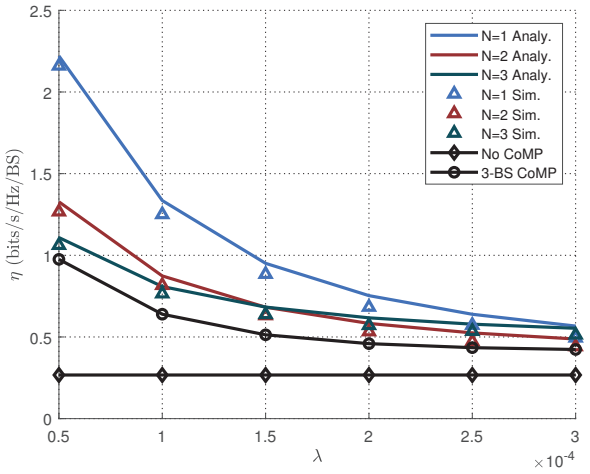

Fig. 3. The normalized spectral efficiency versus λ with different N.

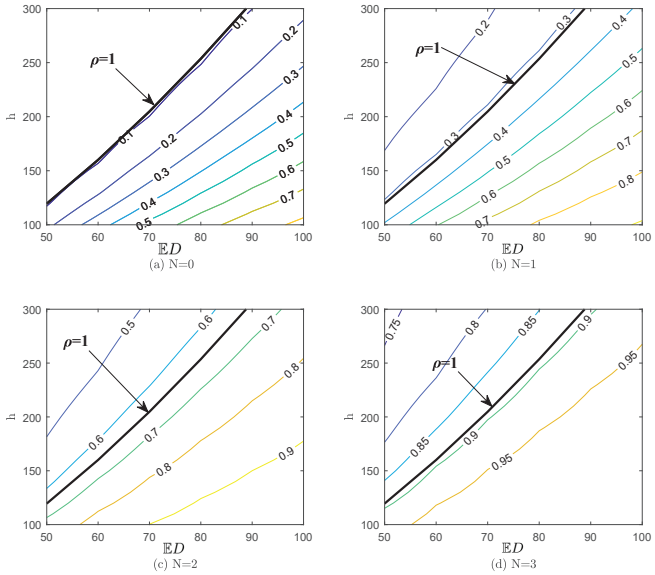

Fig. 4. Contour plots of success probability as a function of $\mathbb{E}D$ and h for different N. The ratio ρ increases as $\mathbb{E}D$ increases or h decreases.

A. Fixed UAV Altitude

Fig. 2 depicts the success probabilities for the typical worst-case user across various scenarios of UAV-BS CoMP with different N, three-BS CoMP and no CoMP. As seen from the plots, the analytical results in Thm. 1 are more consistent with the simulation results than those in Cor. 1. Cor. 1 actually provides an upper bound of the success probability and the gap becomes larger with a larger N. We also observe that the success probability is improved with the increasing N since more BSs participate in the cooperation. Remarkably, even in the scenario with $N = 1$ in the UAV-BS CoMP scheme, the success probability surpasses those of the three-BS CoMP and especially no CoMP scheme. The reason is as follows. Under the parameter setting, we have $\mathbb{E}D = 106$, and thus the average received power from the UAV $\mu_{\mathrm{u}} h^{-\alpha_{\mathrm{u}}}$ is much higher than that from the BS $\mu_{\mathrm{b}} (\mathbb{E}D)^{-\alpha_{\mathrm{b}}}$, which improves the success probability for worst-case users

Fig. 3 demonstrates the normalized spectral efficiency versus the BSs density λ for the air-ground scheme with different N, three-BS CoMP and no CoMP schemes. The alignment between analytical and simulation results affirms the accuracy of our proposed approximations. As λ increases, the normalized spectral efficiency decreases due to the higher interference levels for all the schemes except for the no CoMP scheme. In all cases, the normalized spectral efficiency of UAV-BS CoMP surpasses those of BS CoMP and no CoMP schemes, which shows the effectiveness of UAV-BS CoMP. Additionally, in the case with a small BS density λ, the normalized spectral efficiency of UAV-BS CoMP with $N = 1$ is much higher than the other cases, and its normalized spectral efficiency decreases in the fastest rate with the increase of λ. Thus, the differences between all CoMP curves gradually diminish. This because that for the air-ground link in BS-UAV CoMP, the increase of λ means that both the aggregated interference and the desired signal strength from the coordinated BSs are increased, but the desired signal from the UAV remains unchanged, thus the increasing λ has a larger impact on the UAV-BS CoMP in $N = 1$ than BS CoMP.

B. Effect of BS-UAV Power Ratio

The enhancement of the UAV depends on the ratio of the average powers received from UAV and BSs, defined as $\rho \triangleq \mu_{\mathrm{u}} h^{-\alpha_{\mathrm{u}}} / (\mu_{\mathrm{b}} (\mathbb{E}D)^{-\alpha_{\mathrm{b}}})$, which is a critical parameter of the proposed UAV-BS CoMP scheme. If the UAV power is on average lower than or equal to that of the BSs, it is unnecessary to include the UAV in the cooperative transmission. In Fig. 4, we plot the contour of the success probability for different $\mathbb{E}D$ and h with $T = 0$ dB, and we also add a curve with $\rho(h, \mathbb{E}D) = 1$ on each contour plot, where $N = 0$ means that the worst-cases users are merely served by the UAV. It can be seen that this curve is nearly parallel to the contour curves with a fixed success probability. As $\mathbb{E}D$ increases or h decreases, ρ becomes larger and the success probability is improved due to the UAV assistance. If $\rho \ll 1$, the UAV can hardly help to improve the user-perceived performance.

V. Conclusion

In this paper, a flexible air-ground cooperation scheme was proposed to assist cell-corner users in a Poisson cellular network which stands out for the UAV's adaptability and allows for a dynamic number of coordinated BSs. These users receive the desired signal from the UAV hovering over them and the equidistant nearest BSs with underloaded condition in the non-coherent joint transmission manner. Then we derive the success probability of worst-case users and the normalized spectral efficiency for different number of coordinated BSs. Numerical results show that the proposed scheme outperforms the pure BS CoMP scheme in terms of the success probability and normalized spectral efficiency. Furthermore, the success

probability of the proposed scheme highly depends on the ratio ρ of the average powers received from the UAV and BSs, where a large ρ yields a better performance for worst-case users. In the sparse BS deployment scenario, the air-ground cooperation with one BS has the best normalized spectral efficiency, while the cases with two coordinated BSs and three coordinated BSs have the best one for cell-corner users in the dense deployment scenario, respectively.

ACKNOWLEDGEMENT

This work was supported by the National Natural Science Foundation of China (62371086 and 62201115), the open research fund of State Key Laboratory of Integrated Services Networks (No. ISN24-10), the Aeronautical Science Fund (2022Z001063001), and the U.S. National Science Foundation under Grant 2007498.

APPENDIX A
PROOF OF LEMMA 1

Proof: We first derive the the conditional Laplace transform of $I(t)$, given by

$$\begin{aligned}
&\mathcal{L}_I(s,t) = \mathbb{E}[\exp(-sI(t)) \mid D=t] \\
&= \mathbb{E}\Big[\prod_{x\in\Phi\setminus\mathcal{V}} e^{-s\mu_{\rm b} g_x \ell(\|x\|)} \prod_{y\in\mathcal{V}\setminus\mathcal{W}} e^{-s\mu_{\rm b} g_y \ell(\|y\|)} \mid D=t\Big] \\
&= \mathbb{E}\Big[\prod_{x\in\Phi\setminus\mathcal{V}} e^{-s\mu_{\rm b} g_x \ell(\|x\|)} \mid D=t\Big] \mathbb{E}\Big[\prod_{y\in\mathcal{V}\setminus\mathcal{W}} e^{-s\mu_{\rm b} g_y \ell(\|y\|)} \mid D=t\Big] \\
&= \mathcal{L}_{I_{\rm eq}}(s,t)\mathcal{L}_{I_{re}}(s,t) \qquad (24)
\end{aligned}$$

where

$$\begin{aligned}
\mathcal{L}_{I_{\rm eq}}(s,t) &= \mathbb{E}\Big[\prod_{y\in\mathcal{V}\setminus\mathcal{W}} e^{-s\mu_{\rm b} g_y \ell(\|y\|)} \mid D=t\Big] \\
&= \Big(\frac{1}{1+\mu_{\rm b} s\ell(t)}\Big)^{3-N}, \\
\mathcal{L}_{I_{\rm re}}(s,t) &= \mathbb{E}\Big[\prod_{x\in\Phi\setminus\mathcal{V}} e^{-s\mu_{\rm b} g_x \ell(\|x\|)} \mid D=t\Big] \\
&\overset{(a)}{=} \exp\left(-2\pi\lambda\int_t^\infty \Big(1-\mathbb{E}\big[\exp\left(-s\mu_{\rm b} g_x \ell(r)\right)\big]\Big) r{\rm d}r\right) \\
&= \exp\left(-2\pi\lambda\int_t^\infty \frac{r}{1+\mu_{\rm b}^{-1}s^{-1}\ell^{-1}(r)}{\rm d}r\right). \qquad (25)
\end{aligned}$$

Step (a) follows from the probability generating functional (PGFL) of the PPP [15].

Then through the formula of Leibniz, we can derive the n-th order derivative of $\mathcal{L}_I(s,t)$ w.r.t. s, expressed by

$$\mathcal{L}_I^{(n)}(s,t) = \sum_{k=0}^{n} \binom{n}{k} \mathcal{L}_{I_{\rm re}}^{(n-k)}(s,t) \cdot \mathcal{L}_{I_{\rm eq}}^{(k)}(s,t). \qquad (26)$$

It is easy to obtain the expression of $\mathcal{L}_{I_{\rm eq}}^{(k)}(s,t)$, $k=1,\ldots,n$ through the chain rule of the derivatives. For $\mathcal{L}_{I_{\rm re}}(s,t)$, letting $\eta(s,t) = -2\pi\lambda\int_t^\infty \frac{r}{1+\mu_{\rm b}^{-1}s^{-1}\ell^{-1}(r)}{\rm d}r$, we can observe that $\mathcal{L}_{I_{\rm re}}^{(1)}(s,t) = \eta'(s,t)\mathcal{L}_{I_{\rm re}}(s,t)$, thus according to the formula of Leibniz, we can calculate $\mathcal{L}_{I_{\rm re}}^{(n)}(s,t)$ recursively as follows

$$\mathcal{L}_{I_{\rm re}}^{(n)}(s,t) = \sum_{k=0}^{n-1} \binom{n-1}{k} \eta^{(n-k)}(s,t)\mathcal{L}_{I_{\rm re}}^{(k)}(s,t), \qquad (27)$$

where the k-th order derivative of $\eta(s,t)$ w.r.t. s is

$$\eta^{(k)}(s,t) = 2\pi\lambda(-\mu_{\rm b})^k \int_t^\infty \frac{r^{1-k\alpha_{\rm b}}\Gamma(1+k)}{\big(1+\mu_{\rm b} s\ell(r)\big)^{k+1}}{\rm d}r. \qquad (28)$$

■

REFERENCES

[1] M. S. Ibrahim, A. S. Zamzam, A. Konar, and N. D. Sidiropoulos, "Cell-edge detection via selective cooperation and generalized canonical correlation," *IEEE Transactions on Wireless Communications*, vol. 20, no. 11, pp. 7431–7444, 2021.

[2] Q. Cui, X. Yu, Y. Wang, and M. Haenggi, "The SIR meta distribution in Poisson cellular networks with base station cooperation," *IEEE Transactions on Communications*, vol. 66, no. 3, pp. 1234–1249, 2018.

[3] Y. Zhang, J. Mu, and J. Xiaojun, "Performance of multi-cell mmwave noma networks with base station cooperation," *IEEE Communications Letters*, vol. 25, no. 2, pp. 442–445, 2021.

[4] K. Feng and M. Haenggi, "A location-dependent base station cooperation scheme for cellular networks," *IEEE Transactions on Communications*, vol. 67, no. 9, pp. 6415–6426, 2019.

[5] M. Hua, Q. Wu, D. W. K. Ng, J. Zhao, and L. Yang, "Intelligent reflecting surface-aided joint processing coordinated multipoint transmission," *IEEE Transactions on Communications*, vol. 69, no. 3, pp. 1650–1665, 2021.

[6] Y. Song, S. H. Lim, S.-W. Jeon, and S. Baek, "On cooperative achievable rates of UAV assisted cellular networks," *IEEE Transactions on Vehicular Technology*, vol. 69, no. 9, pp. 9882–9895, 2020.

[7] J. Qi, N. Deng, and H. Wei, "Success probability of Gauss-Poisson UAV-assisted cellular networks with mobility," in *WS14 IEEE ICC 2023 Workshop on Integrating UAVs into 5G and Beyond (WS14 ICC'23 Workshop - UAV5GBynd)*, Rome, Italy, May 2023.

[8] Y. Sun, Z. Ding, and X. Dai, "A user-centric cooperative scheme for UAV-assisted wireless networks in malfunction areas," *IEEE Transactions on Communications*, vol. 67, no. 12, pp. 8786–8800, 2019.

[9] S. Y. Jung, H.-K. Lee, and S.-L. Kim, "Worst-case user analysis in Poisson Voronoi cells," *IEEE Communications Letters*, vol. 17, no. 8, pp. 1580–1583, 2013.

[10] M. Haenggi, "A versatile dependent model for heterogeneous cellular networks," *CoRR*, vol. abs/1305.0947, 2013. [Online]. Available: http://arxiv.org/abs/1305.0947

[11] A. Fotouhi, H. Qiang, M. Ding, M. Hassan, L. G. Giordano, A. Garcia-Rodriguez, and J. Yuan, "Survey on UAV cellular communications: Practical aspects, standardization advancements, regulation, and security challenges," *IEEE Communications Surveys & Tutorials*, vol. 21, no. 4, pp. 3417–3442, Fourth quarter 2019.

[12] R. Tanbourgi, S. Singh, J. G. Andrews, and F. K. Jondral, "A tractable model for noncoherent joint-transmission base station cooperation," *IEEE Transactions on Wireless Communications*, vol. 13, no. 9, pp. 4959–4973, 2014.

[13] R. W. Heath Jr, T. Wu, Y. H. Kwon, and A. C. K. Soong, "Multiuser MIMO in distributed antenna systems with out-of-cell interference," *IEEE Transactions on Signal Processing*, vol. 59, no. 10, pp. 4885–4899, 2011.

[14] H. Alzer, "On some inequalities for the incomplete gamma function," *Mathematics of Computation*, vol. 66, no. 218, pp. 771–778, 1997.

[15] N. Deng, H. Wei, and M. Haenggi, "Modeling and analysis of air-ground integrated networks with flexible beam coverage," *IEEE Transactions on Wireless Communications*, pp. 1–1, 2023.